Available online at www.sciencedirect.com
SCIENCE DIRECT®
Acta Materialia 52 (2004) 1–9
Acta MATERIALIA
www.actamat-journals.com

Taylor hardening in five-power-law creep of metals and Class M alloys

M.E. Kassner *

Materials Science Program, Oregon State University, Rogers Hall, Corvallis, OR 97331, USA

Received 27 May 2003; received in revised form 11 July 2003; accepted 20 August 2003

Abstract

Previous work on aluminum and stainless steel show that the density of dislocations within the subgrain interior (or the network dislocations) are associated with the rate-controlling process for five-power-law creep-plasticity. Furthermore, the hardening in stainless stress is shown to be consistent with the Taylor relation if a linear superposition of "lattice" hardening (τ_o, or the stress necessary to cause dislocation motion in the absence of a dislocation substructure) and the dislocation hardening ($\alpha MGb\rho^{1/2}$) is assumed. It is now shown that the same relationship appears valid for aluminum with the same values of α observed in other metals, where dislocation hardening is established. It appears that the constant, α, is temperature independent and, thus, the dislocation hardening is athermal. It is also shown that constant-stress creep behavior, where the *total* interior dislocation density decreases during primary (hardening stage) creep, is consistent with Taylor hardening.

Keywords: Creep; Dislocation network; Taylor equation

1. Introduction

Steady-state creep (Stage II or secondary creep) is usually described by [1]

$$\dot{\varepsilon}_{ss} = A\left(\frac{\chi}{Gb}\right)^3\left[\frac{D_{sd}Gb}{kT}\right](\sigma_{ss}/G)^n, \quad (1)$$

where the exponent, n, is typically 4–7, D_{sd} is the lattice self-diffusion coefficient, A is a constant, and χ is the stacking fault energy. This equation is applicable above $0.6T_m$. The stress and strain rates refer strictly to steady-state (or secondary, or Stage II) creep plasticity. The steady-state microstructure evolves during primary creep. The dislocations form a three-dimensional subgrain aggregate often characterized by an average subgrain size, λ. Within these subgrains is an (elevated) dislocation density, ρ, usually presumed to form a Frank network. The subgrain boundaries typically have an associated misorientation, θ, of the order of a degree or so, much less than those boundaries of the initial polycrystalline aggregate. It is often assumed that, during steady state, hardening processes are balanced by dynamic recovery processes [1]. It is generally understood that for steady-state structures, λ_{ss} is related to ρ_{ss} and that feature associated with creep resistance or the rate-controlling mechanism for five-power-law creep is not obvious by simple inspection of the microstructures, since both steady-state creep-rate and creep-stress vary predictably with their λ_{ss} and ρ_{ss}.

Most theories for five-power-law creep ($T_m > 0.6T_m$) of pure metals and Class M (or Class I) alloys, that behave similarly to pure metals, rely on some aspect of the subgrain microstructure to describe the rate controlling mechanism. Many of the more recent theories rely on the details of the subgrain boundaries such as the spacing, d, of the dislocations that comprise the boundaries (related to the misorientation angle, θ, across boundaries) or the subgrain size, λ [2–15]. Subgrain boundaries have also been suggested to be the site of elevated long-range internal backstress [16–20] and the rate controlling process at the subgrain boundary has been associated with these

* Present address: Aerospace and Mechanical Engineering, Olin Hall 430, University of Southern California, Los Angeles, CA 90089-1453, USA. Tel.: +1-213-740-7212; fax: +1-213-740-8071.
E-mail address: kassner@usc.edu (M.E. Kassner).

1359-6454/$30.00 © 2003 Acta Materialia Inc. Published by Elsevier Ltd. All rights reserved.
doi:10.1016/j.actamat.2003.08.019

stresses. Other work, however, placed this conclusion of long range internal-stresses in question [21–24]. The dislocations not associated with the subgrain boundaries, which are presumed to form a Frank network, are less commonly, especially recently, claimed to be associated with the rate controlling process of five-power-law creep. Dislocation network theories [1,25–30] generally suppose that the creep behavior is explained in terms of network coarsening by the climb of the nodes and the activation of (critical-sized) links of the network. The acceptance of these models has been limited. This may be somewhat unjustified in view of some careful, and now well-established, experiments. For example, experiments under five-power-law conditions show that there is really no doubt that the elevated temperature flow-stress of AISI 304 stainless steel (Class M alloy) is controlled by the density of dislocations, ρ, not associated with the subgrain boundaries [31]. Also, recent experiments have also shown that the flow properties of high purity aluminum and some (Class A) aluminum alloys under five-power-law creep conditions, appear independent of the subgrain size, λ, or the nature (misorientation) of the subgrain boundaries [32–35].

Traditionally, five-power-law creep theories have necessarily focused on the steady-state or secondary creep behavior. Of course, if a particular feature is associated with the rate controlling process for steady-state five-power-law creep, then the yield stress at a fixed temperature and strain rate (within the five-power-law regime) under non-steady-state conditions would still be expected to be a function of the dimensions of this feature. This is basically equivalent to suggesting that non-steady-state behavior would be determined by the same microstructural features important for steady state. Accordingly, it has been suggested that primary creep and creep transient conditions may obey a relationship,

$$\dot{\varepsilon} = A'\left(\frac{\chi}{Gb}\right)^3 (s)^{p'}[D_{sd}Gb/kT](\sigma/G)^N, \tag{2}$$

where s is a substructural term, originally formulated by Sherby and coworkers [36] to be $(1/\lambda_{ss})$ with $p' \cong 3$. Sherby also suggested that $N = 8$ for aluminum in particular, and, perhaps, other metals as well. It was assumed that the activation energy for (non-steady-state) flow is equal to the activation energy for lattice self-diffusion over the five-power-law regime. Certainly, this equation has been illustrated to have some phenomenological merit, and fairly sophisticated phenomenological equations have been based on this relationship [37]. Sherby and coworkers suggested that the form of Eq. (2) was reasonable since the established relationships [1] between the strengthening variables and the steady-state stress, e.g.,

$$\frac{\sigma_{ss}}{G} = C_1(1/\lambda_{ss})^{-1} \tag{3}$$

or

$$\frac{\sigma_{ss}}{G} = C_2(\rho_{ss})^p, \tag{4}$$

where p is $\cong 0.5$ or

$$\frac{\sigma_{ss}}{G} = d^{-q} \tag{5}$$

when substituted into Eq. (2), would yield the classic five-power-law equation (1). An important question is the nature of the "s" term in Eq. (2) [i.e., ρ, d (or θ), λ]. There may be some problems with this logic, and N not being constant over the five-power-law regime may just be one [1]. Although outside the intended scope of this paper, another complication is that the activation energies in Eqs. (1) and (2) are not necessarily identical.

Consistency with the (modified) Taylor equation [38] is expected if the influence of dislocation density on the flow stress is dominant,

$$\sigma_{T,\dot{\varepsilon}} = \sigma_o + \alpha MGb\rho^{1/2}, \tag{6}$$

where $\sigma_{T,\dot{\varepsilon}}$ is the applied stress at a given temperature and strain rate, G is the shear modulus, b is the Burgers' vector, α is a constant (typically 0.2–0.4 [31,38–42], although the Taylor factor, M, may not always be accurately known in the reported data leaving some uncertainty in this value), and σ_o is the stress required to move a dislocation in the absence of other dislocations that can arise as a result of solutes, Peierls-type stresses, grain-size strengthening, etc. M can vary from 1 (pure shear) to about 3.67 for single crystals and is typically, in tension, 3.06 for polycrystals. This equation was shown to reasonably describe the 304 data within the five-power-law regime by assuming that σ_o was approximately equal to the yield stress of the annealed alloy. Furthermore, the value of α for 304 was within the range observed in other metals at lower temperatures where dislocation hardening is confirmed. In principle, if Eq. (6) is applicable, then the phenomenological relationship of (2) should reduce to the Taylor relationship of Eq. (2).

The first part of this work will demonstrate this same Taylor equation will apply to pure aluminum (with a steady-state structure), having both a much higher stacking fault energy than stainless steel and an absence of substantial solute additions. Second, it will be shown that the microstructure and plastic flow characteristics of aluminum undergoing primary (Stage I) creep under *either* constant-stress or constant strain-rate power-law creep conditions are consistent with Taylor hardening. This latter point is important since it has long been suggested that because the total dislocation density decreases during primary creep *under constant-stress conditions*, the "free" dislocations cannot rationalize hardening during this stage.

2. Analysis

2.1. Steady-state behavior

Fig. 1 shows earlier data [31] by the author where the elevated temperature flow stress of stainless steel is plotted as a function of the square-root of the (total) dislocation density in the subgrain interior. The data reflects steady-state structures as well as specially prepared specimens of stainless steels having various combinations of λ and ρ microstructures produced by utilizing a variety of thermal and mechanical treatments. The specimens were mechanically tested at a given temperature and strain rate that nearly corresponded to the five-power-law creep range. It was found that the (Frank network) dislocation density not associated with subgrain boundaries dominated the strength, described by Eq. (6). Furthermore, as just mentioned, $\alpha = 0.28$, which is consistent with observed values for Taylor hardening of about 0.2–0.4 at ambient temperature for pure metals. Some typical values of from the literature as well as this study are listed in Table 1. One complicating issue with Table 1 is that the value of α is affected by the way ρ is calculated or reported. If ρ is measured as line length per unit volume, then the value of ρ is roughly twice that of ρ reported as intersections per unit area, thus affecting the constant α by a factor of about 1.4. The values by the author for Al and 304 are intersections per unit area, but the units of others of Table 1 are not known. Fig. 7 utilizes line length per unit volume.

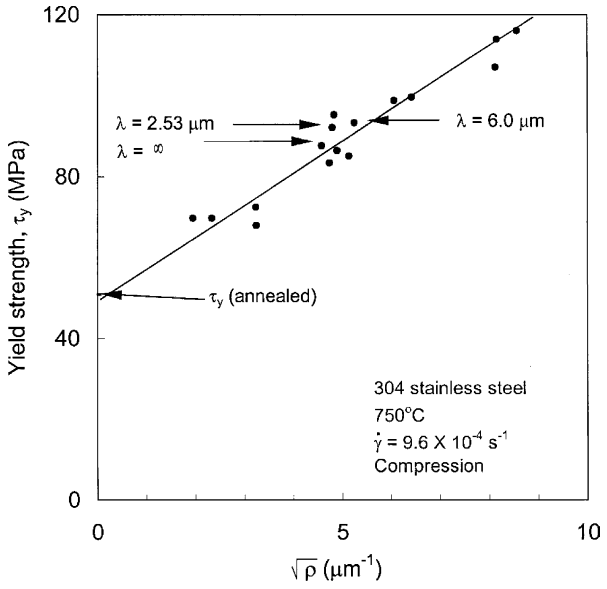

Fig. 1. The elevated temperature yield strength of 304 stainless steel as a function of the square root of the dislocation density (not associated with subgrain boundaries) for specimens of a variety of subgrain sizes. (Approximately five-power-law temperature/strain-rate combination.) Based on [31].

The steady-state flow stress is sometimes described by Eq. (4):

$$\sigma_{ss}/G = C_2(\rho_{ss})^p,$$

where p is an exponent 1–2. Sometimes, p is chosen as 0.5 and

$$\sigma_{ss} = C_2 G(\rho_{ss})^{1/2} \tag{7}$$

(where C is a constant) and the "classic" Taylor equation (e.g., Eq. (6)) has been suggested. However, this relationship between the steady-state stress and the steady-state dislocation density is not for a fixed temperature and strain rate. Hence, it is not of a same type of equation as the classic Taylor equation. That is, this later equation tells us the dislocation density not associated with subgrain boundaries that can be expected for a given steady-state stress which varies with the temperature and strain rate. However, according to Eq. (2), if the strength is *exclusively* provided by ρ, then the strength *is* temperature dependent. Eq. (7) is expected to be athermal [43,44]. Eq. (6), however, contains a temperature dependent σ_o term.

Table 1
Taylor equation α values for various metals

Metal	T/T_m	α [Eq. (6)]	Notes	Ref.
304	0.57	0.28	$\sigma_o \neq 0$, polycrystal	[31]
Cu	0.22	0.34	$\sigma_o = 0$, single crystal 1–6 slip crystal	[38]
Cu	0.22	0.31	$\sigma_o = 0$, polycrystal	[38]
Ti	0.15	0.37	$\sigma_o \cong 0.25$–0.75 flow stress Polycrystal	[39]
Ag	0.24	0.19–0.34	Stages I and II single crystal $M = 1.78$–1 $\sigma_o \neq 0$	[40]
Ag	0.24	0.31	$\sigma_o = 0$, polycrystal	[41]
Al	0.51–0.83	0.20	$\sigma_o \neq 0$, polycrystal	This study
Fe	–	0.23	$\sigma_o \neq 0$, polycrystal	[38]

Note: α values of Al and 304 stainless stress are based on dislocation densities of intersections per unit area. The units of the others are not known and these values would be adjusted lower by a factor of 1.4 if line-length per unit volume is utilized.

A similar experiment illustrated in Fig. 1 has also been performed on steady-state structures of aluminum [36,45]. In one case [36], aluminum specimens were deformed to various steady state stresses at a given temperature by varying the applied strain rate. The strain rate was quickly changed to a common strain rate after steady state was achieved and the new plastic flow stress (at a fixed temperature and strain rate) was noted. The subgrain sizes were measured at each steady state, so that the dependence of the flow stress at a specific temperature and strain rate on the subgrain size could be determined. Eq. (2) was basically formulated based on these experiments. In another case [45] three specimens were deformed at various temperatures and strain rates, again, to steady state. The specimens were quickly cooled to 300 °C and re-deformed at a fixed strain rate. The new flow stress (again, at a fixed temperature and strain rate) was also related to the measured (steady state) subgrain sizes produced at the higher temperatures. The data in both cases suggests a phenomenological relationship between the flow stress at a fixed temperature and strain rate and the (steady state) subgrain size (the network or the dislocation density within the subgrain was not considered):

$$\sigma_{T,\dot{\varepsilon}} = \sigma_o + k_1(1/\lambda_{ss})^{0.7}, \tag{8}$$

where k_1 is a constant. It should be noted that the σ_o term is a *substantial* fraction of the steady-state flow curve (as illustrated subsequently) despite the high purity (also see Fig. 6(a)). Thus a "friction stress" unrelated to dislocation hardening is still appropriate, just as with the stainless steels case. Again, the two phenomenological equations (2) and (8), in principle, are equivalent at a fixed temperature and strain rate.

Eq. (3) is based on steady-state deformation. Since the steady-state subgrain size is generally related to the steady-state dislocation density ρ_{ss},

$$(1/\lambda_{ss}) = K''(\rho_{ss})^p, \tag{9}$$

where, as pointed out earlier, p may vary from 1 to 2 [1]. Hofmann and Blum's [46] careful measurements suggest a value of about 1.6. Substituting Eq. (9) into Eq. (8) suggests that for steady-state structures of aluminum (deforming under a non-steady-state "reference" temperature and strain rate),

$$\sigma_{T,\dot{\varepsilon}} = \sigma_o + \alpha' MGb\rho^{0.43}, \tag{10}$$

where σ_o is roughly the yield stress of the annealed aluminum at the reference temperature and strain rate. This suggests that the same classic Taylor equation that can be used to describe elevated temperature dislocation hardening in stainless steel is applicable here, as well. An important additional question to assess the validity of the Taylor equation is to modify the dislocation density exponent to 0.5 in Eq. (10) and assess the value of α. If both the phenomenological description of the influence of the strength of dislocations in high purity metals such as aluminum have the form of the Taylor equation and *also* have the expected values for the constants, then it would appear that the elevated temperature flow stress is provided by the Frank network rather than subgrain walls.

Fig. 2 plots modulus-compensated steady-state stress versus diffusion-coefficient-compensated steady-state strain rate. Fig. 3 illustrates the well-established trend between the steady-state dislocation density (line length per unit volume) and the steady-state stress. The steady-state flow stress can be predicted at a reference strain rate (e.g., 5×10^{-4} s^{-1}), at a variety of temperatures, with an associated steady-state dislocation density from these two figures. If Eq. (6) is valid, then the values for α could be calculated for each temperature, by assuming that the annealed dislocation density and the σ_o values account for the annealed yield strength measured in this study and reported in Fig. 4.

Fig. 4 reports new experiments by the author while Figs. 6 and 8 were produced by the author and coworkers in previously reported experiments [31,33]. The experimental details of these experiments are carefully described in these references. The Al specimens are all of 99.999% purity and annealed at 425 °C in vacuum prior to testing. All mechanical tests were performed at a strain rate of 5×10^{-4} s^{-1}. The grain sizes of tests reported in Fig. 4 were about 1 mm while those reported in Figs. 6 and 8 were about 1/4–1/2 mm. Specimen sizes were 25.4 mm gage length and 5.1–6.4 mm dia. Grain and subgrain sizes for the author's (and the other investigations reported in the other figures) data are based

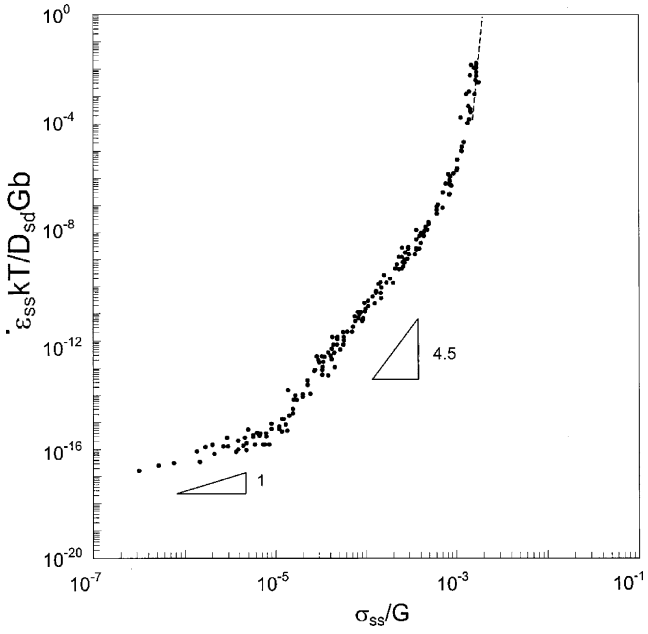

Fig. 2. The compensated steady-state strain rate versus the modulus compensated steady-state stress for 99.999 pure Al, based on [59].

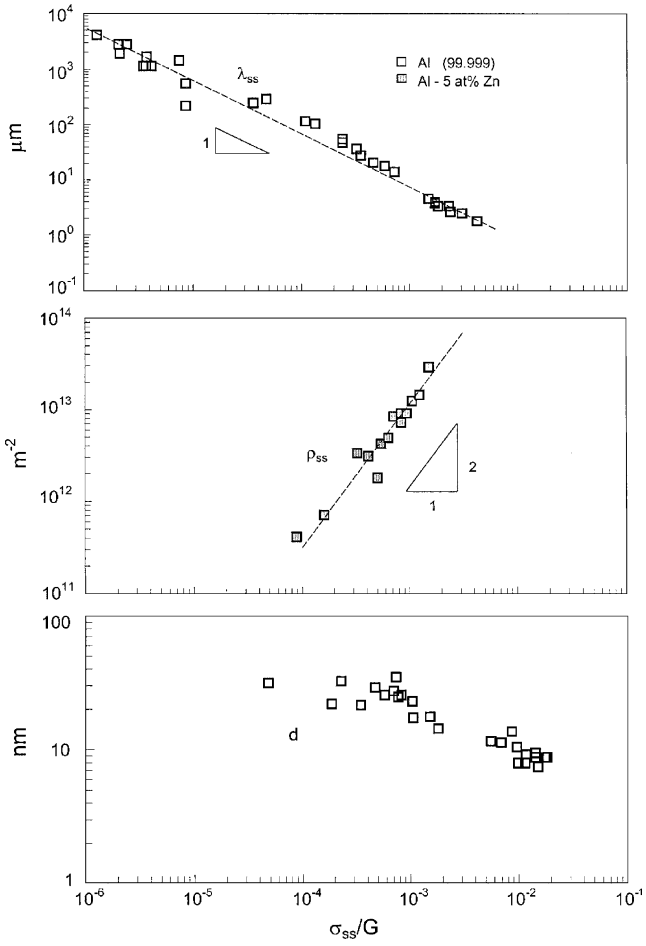

Fig. 3. The average steady-state subgrain intercept, λ, density of dislocations not associated with subgrain walls, ρ, and the average separation of dislocations that comprise the subgrain boundaries for Al (and Al–5 at.% Zn that behaves, mechanically, essentially identical to Al, but is suggested to allow for a more accurate determination of ρ by TEM). Based on [60].

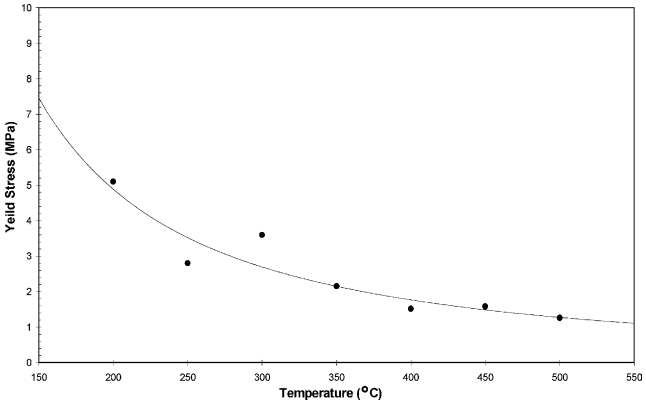

Fig. 4. The tensile (0.2% offset) yield strength of 99.999% pure Al as a function of temperature at $\dot{\varepsilon} = 5 \times 10^{-4}$ s^{-1}.

on an average line intercept. Dislocation densities are reported using a surface intersection technique under $g< 220 >$ two-beam conditions in the TEM, where

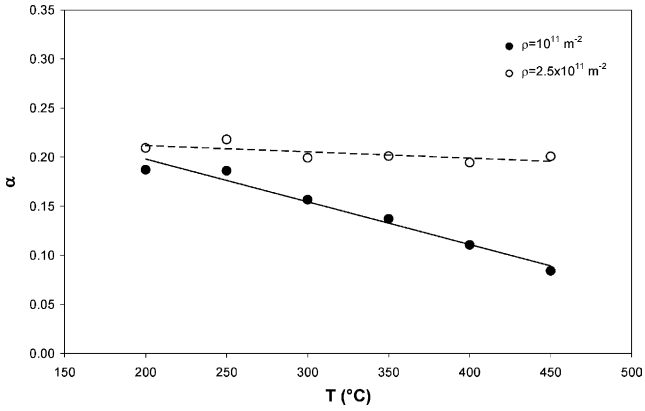

Fig. 5. The values of the constant α in the Taylor equation (6) as a function of temperature. The alpha values depend somewhat on the assumed annealed dislocation density. Hollow dots, $\rho = 2.5 \times 10^{11}$ m^{-2}; solid, $\rho = 10^{11}$ m^{-2}.

about 5/6 of all dislocations are imaged. Dislocation densities were taken at foil thicknesses of 1 μm in order to minimize dislocation escape from the foil. TEM thin-foil specimen preparation techniques avoided any damage that could introduce artifact dislocations.

Fig. 5 reports the resulting α values. Fig. 5 indicates, first, that typical values of α are within the range of those expected for Taylor strengthening. Said another way, strengthening of (steady state) structures can be reasonably predicted based on a Taylor equation. The strength we predict, based only on the (network) dislocation density and completely independent of the heterogeneous (subgrain) dislocation substructure. This point is consistent with the observation that the elevated-temperature yield strength of annealed, polycrystalline aluminum [high-angle boundaries (HABs) only] is essentially independent of the grain size [47]. It has further been established that for a fixed grain size/subgrain size, the flow stress is independent of large variations in the misorientation [33]. Furthermore, the values of α are completely consistent with the values of α in other metals (at high and low temperatures) in which dislocation hardening is established (see Table 1). The fact that the higher temperature α values of Al and 304 stainless steel are consistent with the ambient-temperature values is consistent with the athermal behavior of Fig. 5. The non-near-zero annealed dislocation density observed experimentally may be consistent with Ardell et al. suggestion of network frustration creating a lower limit to the dislocation density.

One point to note is that in Fig. 5 the variation in α with temperature depends on the value selected for the annealed dislocation density. For a value of 2.5×10^{11} m^{-2}, the values of the alpha constant are nearly temperature independent, suggesting that the dislocation hardening is, in fact, theoretically palatable in that it is athermal. The annealed dislocation density for which athermal behavior is observed is that which is very

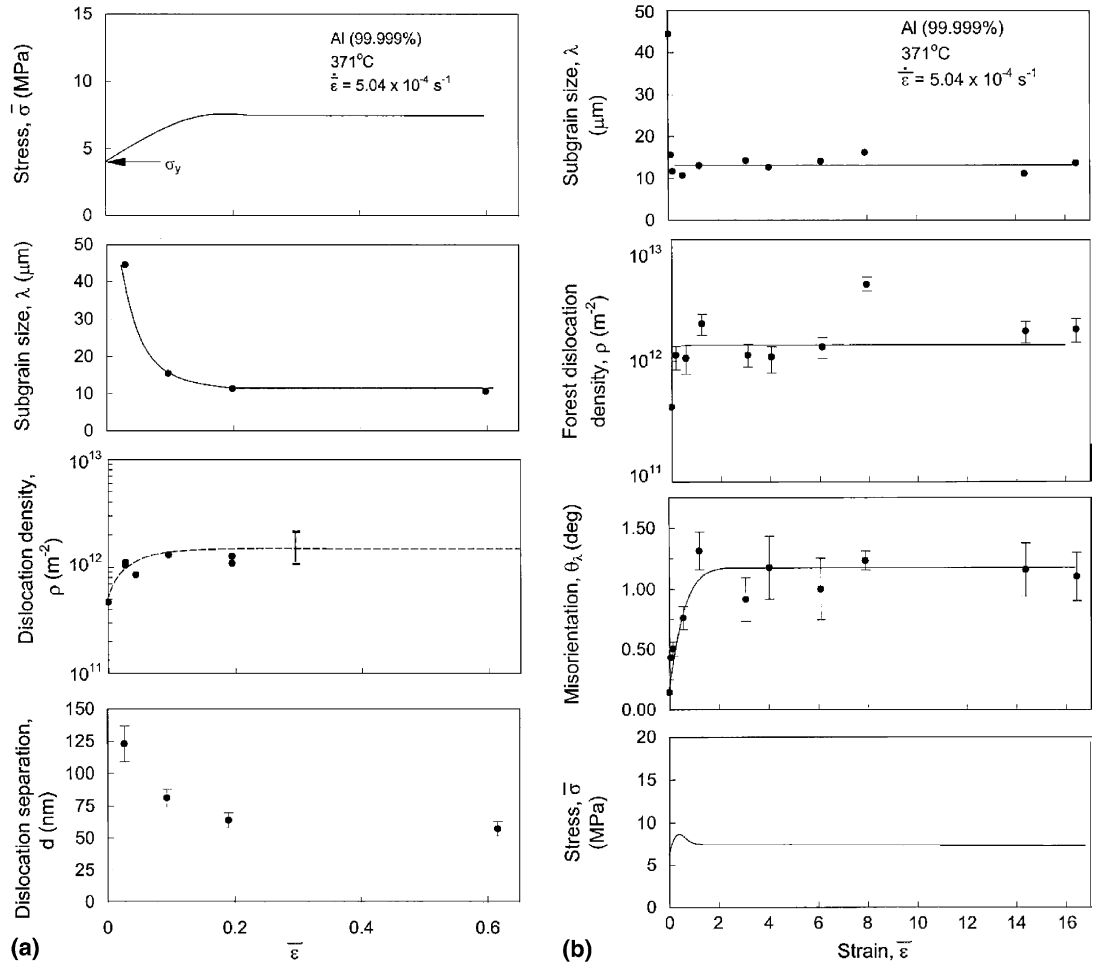

Fig. 6. The work-hardening at a constant strain-rate creep transient for Al illustrating the variation of λ, ρ, d, and $\theta_{\lambda_{ave}}$ over primary and secondary creep. The bracket refers to the range of steady-state dislocation density values observed at larger strains [e.g., see (b)]. From [33].

close to the value observed by the author (Fig. 6), and suggested by Blum [48]. The suggestion of athermal dislocation hardening is consistent with the model by Nes [44], where, as in the present case, the temperature dependence of the constant (or fixed dislocation substructure) structure flow stress is provided by the important temperature-dependent σ_o term.

It perhaps should be mentioned that if it is assumed both that $\sigma_o = 0$ and that the dislocation hardening is athermal [i.e., Eq. (7) is "universally" valid] then α is about equal to 0.53, or about a factor of two larger than anticipated for dislocation hardening. Hence, aside from not including a σ_o term which allows temperature-dependence, the alpha term appears somewhat large.

2.2. Primary creep behavior

The trends in dislocation density during primary creep have been less completely investigated for the case of constant strain-rate tests than constant-stress creep tests. Earlier work by the author [31] on 304 stainless steel found that at $0.57T_m$ (and the same strain rates as Fig. 1), the increase in flow stress by a factor of three is associated with increases in dislocation density with strain that are consistent with the Taylor equation. That is, the ρ versus strain and stress versus strain give a σ versus ρ that "falls" on the line of Fig. 1 [49]. Similarly, the aluminum primary transient in Fig. 6, where the dislocation density monotonically increases to the steady-state value under constant *strain-rate* conditions, can also be shown consistent with the Taylor equation.

Challenges to the proposition of Taylor hardening for 5-power-law creep in metals and Class M alloys include the microstructural observations during primary creep under constant-*stress* conditions. For example, it has nearly always been observed during primary creep of pure metals and Class M alloys that the density of dislocations not associated with subgrain boundaries increases from the annealed value to a peak value, but then gradually decreases to a steady-state value that is between the annealed and the peak density [50–55] (e.g., Fig. 7). Typically, the "peak" dislocation density value, ρ_p, measured at a strain level that is roughly one-fourth of the strain required to attain steady state ($\varepsilon_{ss}/4$), is a

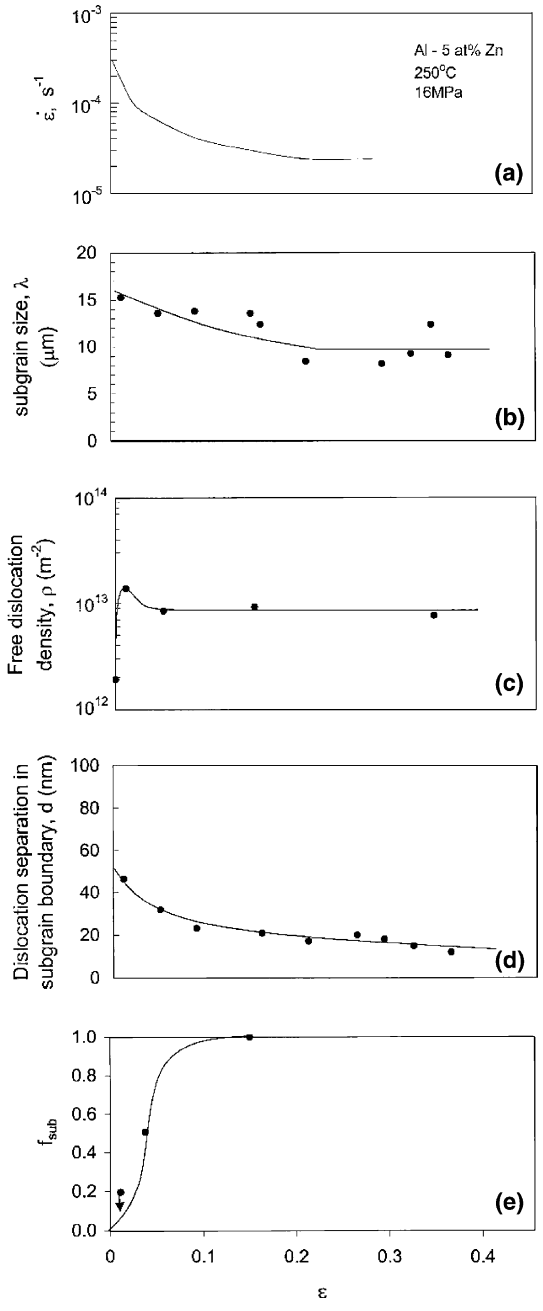

Fig. 7. The constant-stress primary creep transient in Al–5 at.% Zn (essentially identical behavior to pure Al) illustrating the variation of the average subgrain intercept, λ, density of dislocations not associated with subgrain walls, ρ, and the spacing, d, of dislocations that comprise the boundaries. The fraction of material occupied by subgrains is indicated by f_{sub}. The subgrain size during primary creep reflects those regions of the grain where subgrain formation is observed. Based on [61].

factor of 1.5–4 higher than the steady-state ρ_{ss} value. It was believed, by some, difficult to rationalize hardening by network dislocations if the overall density is decreasing while the strain rate is decreasing. Therefore, an important question is whether the Taylor hardening, observed under constant strain-rate conditions, is consistent with this observation. This behavior could be interpreted as evidence that most of these dislocations have a dynamical role rather than a (Taylor) hardening role, since the initial strain rates in constant-stress tests may require by the equation,

$$\dot{\varepsilon} = (b/M)\rho_{\text{m}} v \tag{11}$$

a high mobile (nonhardening) dislocation density, ρ_{m}, that gives rise to high initial values of total density of dislocations not associated with subgrain boundaries, ρ, where v is the dislocation velocity. That is, of the total density of dislocations not associated with subgrain boundaries, at any instant, some are mobile (ρ_{m}) while some are obstacles, perhaps as links of the Frank network ($\rho - \rho_{\text{m}}$). As steady state is achieved and the strain rate decreases, so does ρ_{m} and in turn, ρ.

More specifically, Taylor hardening during primary constant-stress creep may be valid based on the following argument:

From Eq. (11) $\dot{\varepsilon} = \rho_{\text{m}} v b/M$. We assume [56]

$$v = k_1 \sigma^1 \tag{12}$$

and, therefore, for constant strain-rate tests,

$$\dot{\varepsilon}_{\text{ss}} = [k_1 b/M]\rho_{\text{m}}\sigma. \tag{13}$$

The ε_{p} (plastic strain) is small at the onset of yielding in a constant strain-rate test ($\dot{\varepsilon} = \dot{\varepsilon}_{\text{ss}}$), and there is only minor hardening, and the mobile dislocation density is a fraction, f_{m}^{o}, of the total density,

$$f_{\text{m}}^{\text{o}}\rho_{(\varepsilon_{\text{p}}=0)} = \rho_{\text{m}(\varepsilon_{\text{p}}=0)}$$

therefore, for aluminum (see Fig. 6)

$$\rho_{\text{m}(\varepsilon_{\text{p}}=0)} = f_{\text{m}}^{\text{o}} 0.64\rho_{\text{ss}} \quad \text{(based on } \rho \text{ at } \varepsilon_{\text{p}} = 0.03), \tag{14}$$

where f_{m}^{o} is basically the fraction of dislocations in the annealed metal that are mobile at the yield stress (half the steady-state flow stress) in a constant strain-rate test. Also from Fig. 6, $\sigma_y/\sigma_{\text{ss}} = 0.53$. Therefore, at small strains,

$$\dot{\varepsilon}_{\text{ss}} = f_{\text{m}}^{\text{o}} 0.64(0.53)[k_1 b/M]\rho_{\text{ss}}\sigma_{\text{ss}} \tag{15}$$

(constant strain rate at $\varepsilon_{\text{p}} = 0.03$).

At steady state, $\sigma = \sigma_{\text{ss}}$ and $\rho_{\text{m}} = f_{\text{m}}^{\text{s}}\rho_{\text{ss}}$, where f_{m}^{s} is the fraction of the total dislocation density that is mobile at steady state and

$$\dot{\varepsilon}_{\text{ss}} = f_{\text{m}}^{\text{s}}[k_1 b/M]\rho_{\text{ss}}\sigma_{\text{ss}} \tag{16}$$

(constant strain rate at $\varepsilon_{\text{p}} > 0.20$).

By combining Eqs. (15) and (16) we find that f_{m} at steady state is about 1/3 the fraction of mobile dislocations in the annealed polycrystals ($0.34 f_{\text{m}}^{\text{o}} = f_{\text{m}}^{\text{s}}$). This suggests that during steady state only 1/3, or less, of the total dislocations (not associated with subgrain boundaries) are mobile and the remaining 2/3, or more, participate in hardening. The finding that a large fraction are immobile is consistent with the observation that increased dislocation density is associated with increased

strength for steady-state deformation and constant strain-rate testing. Of course, there is the assumption that the stress acting on the dislocations as a function of strain (microstructure) is proportional to the applied flow stress. This is sensible (and the fraction is probably unity) for a network model. Furthermore, we have presumed a 55% increase in ρ over primary creep with some uncertainty in the density measurements.

For the constant-stress case we again assume

$$\dot{\varepsilon}_{\varepsilon_p\cong 0} = f_m^p[k_1 b/M]\rho_p\sigma_{ss} \quad \text{(constant stress)}, \tag{17}$$

where f_m^p is the fraction of dislocations that are mobile at the peak (total) dislocation density of ρ_p, the peak dislocation density, which will be assumed equal to the maximum dislocation density observed experimentally in a ρ–ε plot of a constant-stress test. Since at steady state from Eq. (15),

$$\dot{\varepsilon}_{ss} \cong 0.34 f_m^o[k_1 b/M]\rho_{ss}\sigma_{ss}$$

by combining with Eq. (17),

$$\dot{\varepsilon}_{\varepsilon_p\cong 0}/\dot{\varepsilon}_{ss} = \left(\frac{f_m^p}{f_m^o}\right)3\rho_p/\rho_{ss} \quad \text{(constant stress)} \tag{18}$$

(f_m^p/f_m^o) is not known but if we assume that at macroscopic yielding, in a constant strain-rate test, for annealed metal, $f_m^o \cong 1$, then we might also expect at small strain levels and relatively high dislocation densities in a constant-stress test, $f_m^p \cong 1$. This would suggest that fractional decreases in $\dot{\varepsilon}$ in a constant-stress test are not equal to those of ρ. This apparent contradiction to purely dynamical theories (i.e., based strictly on Eq. (11)) is reflected in experiments [50,51,53,55] where the kind of trend predicted in Eq. (18) is in fact observed. Eq. (18) and the observations of $\dot{\varepsilon}$ against ε in a constant-stress test at the identical temperature can be used to roughly predict the expected constant stress ρ–ε curve in aluminum at 371 °C and about 7.8 MPa; the same conditions as the constant strain-rate test of Fig. 6. If we use small plastic strain levels (i.e., $\varepsilon \cong \varepsilon_{ss}/4$, where ρ values have been measured in constant-stress tests), we can determine the ratio (e.g., $\dot{\varepsilon}_{\varepsilon=(\varepsilon_{ss}/4)}/\dot{\varepsilon}_{\varepsilon=\varepsilon_{ss}}$) in constant-stress tests. This value seems to be roughly 6 at stresses and temperatures comparable to Fig. 6 [11,50,51,57,58]. This ratio was applied to Eq. (18) [assuming $(f_m^p/f_m^c) \cong 1$]; the estimated ρ–ε trends, in a constant-stress test in Al at 371 °C, are shown in Fig. 8. This estimate, which predicts a peak dislocation density of $2.0\rho_{ss}$, is consistent with the general observations discussed earlier for pure metals and Class M alloys, that ρ_p is between $1.5\rho_{ss}$ and $4\rho_{ss}$ (1.5–2.0 for aluminum). Thus, the peak-behavior observed in the dislocation density versus strain trends, which at first glance appear to impugn dislocation network hardening, is, actually, consistent, in terms of the observed ρ values, to Taylor hardening.

Two particular imprecisions in the argument above are that it was assumed (based on some experimental work in the literature) that the stress exponent for the elevated temperature (low stress) dislocation velocity, v, is one. This exponent may not be well known and may be greater than 1. The ratio (ρ_p/ρ_{ss}) is multiplied from a value of 3 in Eq. (18) to higher values of $3[2^{n-1}]$, where n is defined by $v = \sigma^n$. This means that the observed strain-rate "peaks" would predict smaller dislocation peaks or even an absence of peaks for the observed initial strain rates in constant-stress tests. In a somewhat circular argument, the consistency between the predictions of Fig. 8 and the experimental observations may suggest that the exponents of 1–2 may be reasonable. Also, the values of the peak dislocation densities and strain rates are not unambiguous, and this creates additional uncertainty in the argument.

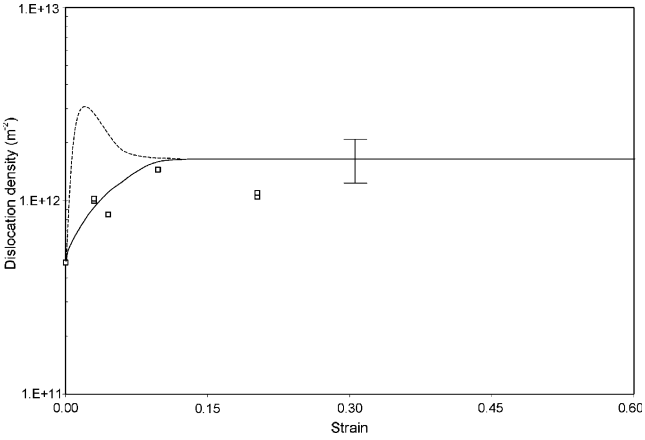

Fig. 8. The predicted dislocation density (– – –) in the subgrain interior against strain for aluminum deforming under constant-stress conditions is compared with that for constant strain-rate conditions (—). The predicted dislocation density is based on Eq. (18) which assumes Taylor hardening.

3. Summary

Previous work on aluminum and stainless steel show that the density of dislocations within the subgrain interior influences the flow stress for steady-state substructures and primary creep under constant strain-rate conditions. The hardening is consistent with the Taylor relation if a linear superposition of solute/lattice hardening (σ_o, or the stress necessary to cause dislocation motion in the absence of a dislocation substructure) and the dislocation hardening ($\cong \alpha MGb\rho^{1/2}$) is assumed. Here is assumed that the fraction of immobile dislocations ($\rho - \rho_m$) is a constant fraction of the total dislocation density. It appears that the constant, α, is temperature independent and, thus, the dislocation hardening is athermal. Furthermore, it is shown that constant-stress creep behavior where the *total* dislocation density (ρ) decreases during primary (hardening

stage) creep, is actually consistent with Taylor hardening. The increase in total dislocation density simply reflects the high initial strain rates in a constant-stress test. The obstacles for dislocation motion in this case are still the network dislocations.

Acknowledgements

This work was supported by Basic Energy Sciences, US Department of Energy, under grant DE-FG03-99ER45768. The mechanical testing by Dr. M.-Z. Wang and Kevin Kyle is greatly appreciated. The comments to this manuscript by Prof. W. Blum are appreciated.

References

[1] Kassner ME, Perez-Prado MT. Prog Mater Sci 2000;45:1.
[2] Morris MA, Martin JL. Acta Metall 1984;32:1609.
[3] Morris MA, Martin JL. Acta Metall 1984;32:549.
[4] Derby B, Ashby MF. Acta Metall 1987;35:1349.
[5] Nix WD, Ilschner B. In: Haasen P, Gerold V, Kostorz G, editors. Strength of metals and alloys. Oxford: Pergamon; 1980. p. 1503.
[6] Straub S, Blum W, Maier HJ, Ungar T, Borberly A, Renner H. Acta Mater 1996;44:4337.
[7] Argon AS, Takeuchi S. Acta Metall 1981;29:1877.
[8] Gibeling JC, Nix WD. Acta Metall 1980;29:1769.
[9] Blum W, Cegielska A, Rosen A, Martin JL. Acta Metall 1989;37:2439.
[10] Hasegawa T, Ikeuchi Y, Karashima S. Metal Sci 1972;6:78.
[11] Ginter TJ, Mohamed FA. J Mater Sci Eng 1982;17:2007.
[12] Barrett CR, Nix WD, Sherby OD. Trans ASM 1966;59:3.
[13] Blum W, Hausselt J, König G. Acta Metall 1976;24:293.
[14] Weertman J. In: Wilshire B, editor. Creep and fracture of engineering materials and structures. Swansea: Pineridge; 1984. p. 1.
[15] Maruyama K, Karachima S, Oikawa H. Res Mech 1983;7:21.
[16] Mughrabi H. Acta Metall 1983;31:1367.
[17] Borbély A, Blum W, Ungar T. Mater Sci Eng 2000;276:186.
[18] Borbély A, Hoffmann G, Aernoudt E, Ungar T. Acta Mater 1997;45:89.
[19] Lepinoux J, Kubin LP. Phil Mag A 1985;57:675.
[20] Mughrabi H, Ungar T. In: Nabarro FRN, editor. Dislocations in solids. North Holland, in press.
[21] Sleeswyk AW, James MR, Plantinga DH, Maathuis WST. Acta Metall 1978;l26:1265.
[22] Kassner ME, Pérez-Prado MT, Vecchio KS, Wall MA. Acta Mater 2000;48:4247.
[23] Orowan E. Internal stress and fatigue in metals. In: General Motors Symposium; 1959. Amsterdam: Elsevier. p. 59.
[24] Gaal I. In: Andersen NH, Eldrup M, Hansen N, Juul Jensen D, Leffers T, Lilholt H, Pedersen OB, Singh BN, editors. Proc 5th Inter Riso Symp. Roskilde (DK): Riso National Lab; 1984. p. 249.
[25] Ostrom P, Lagneborg R. Res Mech 1980;1:59.
[26] Kassner ME, Pérez-Prado MT, Long M, Vecchio KS. Metall Mater Trans A 2002;33:311.
[27] Ardell AJ, Przystupa M. Mech Mater 1984;4:319.
[28] Evans HE, Knowles G. Acta Metall 1977;25:963.
[29] McLean D. Trans AIME 1968;22:1193.
[30] Przystupa MA, Ardell AJ. Metall Mater Trans A 2002;33:231.
[31] Kassner ME. J Mater Sci 1990;25:1997.
[32] Kassner ME. Mater Sci Eng 1993;166:81.
[33] Kassner ME, McMahon ME. Metall Trans A 1987;18:835.
[34] Doherty RD, Hughes DA, Humphreys FJ, Jonas JJ, Juul Jensen D, Kassner ME, King WE, McNelley TR, McQueen HJ, Rollett AD. Mater Sci Eng 1997;A238:219.
[35] McQueen HJ, Evangelista E, Kassner ME. Z Metall 1991;82:336.
[36] Young CM, Robinson SL, Sherby OD. Acta Metall 1975;23:633.
[37] Miller AK. Constitutive equations for creep and plasticity. Essex, UK: Elsevier Applied Science; 1987.
[38] Widersich H. J Metals 1963:423.
[39] Jones RL, Conrad H. TMS–AIME 1969;245:779.
[40] Levinstein HJ, Robinson WH. The relations between structure and the mechanical properties of metal. In: Symp. at the National Physical Lab, January 1963. Her Majesty's Stationery Office, p. 180. From : Weertman J, Weertman JL. In: Cahn RW, Hassen P, editors. Physical Metallurgy. Elsevier, 1983. p. 1259.
[41] Bailey JE, Hirsch PB. Phil Mag 1960;5:485.
[42] Taylor GI. Proc Roy Soc 1934;A145:362.
[43] Weertman J. Mechanics and materials interlinkage. New York: J. Wiley; 1999. p. 451.
[44] Nes E. Prog Mater Sci 1997;41:129.
[45] Kuchi SK, Yamaghuchi A. In: McQueen HJ, Baillon JP, Dickson JI, Jonas JJ, Akben MG, editors. Strength of metals and alloys. Oxford: Pergamon; 1985. p. 899.
[46] Hofmann U, Blum W. In: 7th Inter Symp on Aspects of High Temperature Deformation and Fracture of Crystalline Materials. Sendai: Jap. Inst. Metals; 1993. p. 625.
[47] Kassner ME, Li X. Scripta Met Mater 1991;25:2833.
[48] Blum W. Private communication, 2002.
[49] Kassner ME, Miller AK, Sherby OD. Metall Trans 1982;13A:1977.
[50] Blum W, Absenger A, Feilhauer R. In: Haasen P, Gerold V, Kostorz G, editors. Strength of metals and alloys. Oxford: Pergamon; 1980. p. 265.
[51] Daily S, Ahlquist CN. Scripta Metall 1972;6:95.
[52] Sikka VK, Nahm H, Moteff J. Mater Sci Eng 1975;20:95.
[53] Orlova A, Pahutova M, Cadek J. Phil Mag 1972;25:865.
[54] Stang RG, Nix WD, Barrett CR. Metall Trans 1971;2:1233.
[55] Clauer AH, Wilcox BA, Hirth JP. Acta Metall 1970;18:381.
[56] Gorman JA, Wood DS, Vreeland T. J Appl Phys 1969;40:833.
[57] Parker JD, Wilshire B. Mater Sci Eng 1980;43:271.
[58] Raymond L, Dorn JE. Trans AIME 1964;230:560.
[59] Straub S, Blum W. Scripta Met Mater 1990;24:1837.
[60] Blum W. In: Cahn RW, Haasen P, Kramer ES, Mughrabi H, editors. Materials science and technology, vol. 6. Wienheim: Verlag Chemie; 1993. p. 339.
[61] Blum W. In: Langdon TG, Merchant HD, Morris JG, Zaidi MA, editors. Hot deformation of aluminum alloys. TMS; 1991. p. 181.